Fisheye Lenses Calibration Using Straight-Line Spherical Perspective Projection Constraint

Xianghua Ying[1,⋆], Zhanyi Hu[2], and Hongbin Zha[1]

[1] National Laboratory on Machine Perception, Peking University, Beijing, P.R. China
{xhying, zha}@cis.pku.edu.cn
http://www.cis.pku.edu.cn/vision/Visual&Robot/people/ying/
[2] National Laboratory of Pattern Recognition, Institute of Automation, Chinese Academy of Sciences
huzy@nlpr.ia.ac.cn

Abstract. Fisheye lenses are often used to enlarge the field of view (FOV) of a conventional camera. But the images taken with fisheye lenses have severe distortions. This paper proposes a novel calibration method for fisheye lenses using images of space lines in a single fisheye image. Since some fisheye cameras' FOV are around 180 degrees, the spherical perspective projection model is employed. It is well known that under spherical perspective projection, straight lines in space have to be projected into great circles in the spherical perspective image. That is called straight-line spherical perspective projection constraint (SLSPPC). In this paper, we use SLSPPC to determine the mapping between a fisheye image and its corresponding spherical perspective image. Once the mapping is obtained, the fisheye lenses is calibrated. The parameters to be calibrated include principal point, aspect ratio, skew factor, and distortion parameters. Experimental results for synthetic data and real images are presented to demonstrate the performances of our calibration algorithm.

1 Introduction

In many computer vision applications, including robot navigation, 3D reconstruction, image-based rendering, and single view metrology, a camera with a quite large field of view (FOV) is preferable. A conventional camera has a very limited FOV. Therefore, cameras with wide-angle or fisheye lenses are often employed. Images taken with these imaging devices often have significant distortions. If we want to use some perspective information from these distorted images, they have to be transformed into perspective images. A fisheye camera's FOV is around 180 degrees, but a wide-angle camera's FOV is usually around 100 degrees. The existing calibration methods [2, 4, 5, 9] for wide-angle camera using images of space lines cannot be directly used for fisheye cameras. Therefore, this paper aims at calibrating fisheye cameras using images of space lines. An image from a fisheye camera with FOV 183 degrees (Nikon COOLPIX 990 with FC-E8 fisheye lenses) is shown in Fig. 1a.

⋆ This work was partially carried out while the author was at the Chinese Academy of Sciences.

P.J. Narayanan et al. (Eds.): ACCV 2006, LNCS 3852, pp. 61–70, 2006.

(a)

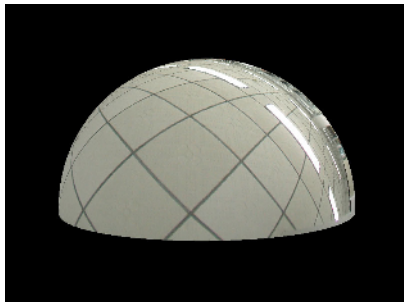

(b)

Fig. 1. (a) A fisheye image. (b) The corresponding spherical perspective projection image. The calibration procedure is to find the mapping between those two.

In literature, there are two standard types of perspective images used in computer vision: planar and spherical surfaces (i.e., a planar or a spherical surface can be used as the retina of a perspective camera). Due to lens distortions, space lines are projected into image curves in the actual image. Once the mapping between a distorted image and its corresponding perspective image is obtained, the calibration problem is solved. The mapping can be obtained by finding the relation between the image curves of space lines and its corresponding perspective images. It is well known that under planar perspective projection, images of straight lines in space have to be mapped into straight lines in the planar perspective image. That is called the straight-line planar perspective projection constraint (SLPPPC). The existing calibration methods [2, 4, 5, 9] for wide-angle cameras using the distorted images of lines are all based on SLPPPC. However, for fisheye cameras with FOV around 180 degrees, we use the spherical perspective projection model because it is a convenient way to represent FOV around 180 degrees. We also know that under spherical perspective projection, images of straight lines in space have to be projected into great circles in the spherical perspective image. Therefore, there exists another constraint we called the straight-line spherical perspective projection constraint (SLSPPC). In this paper we elaborate on how to determine the mapping between a fisheye image and its corresponding spherical perspective image using SLSPPC (see Fig. 1).

2 Fisheye Imaging Model

Fisheye imaging model describes a mapping from 3D space points to 2D fisheye image points (see Fig. 2). We introduce the spherical perspective projection into the fisheye imaging model and divide the imaging model into four concatenated steps as follows:

Step 1: Transform the 3D world coordinates of a space point into the 3D camera coordinates.

Considering a generic 3D point, visible by a fisheye camera, with Cartesian coordinates $\mathbf{P}_W = (X, Y, Z)^T$ in the world coordinate system, if $\mathbf{P}_C =$

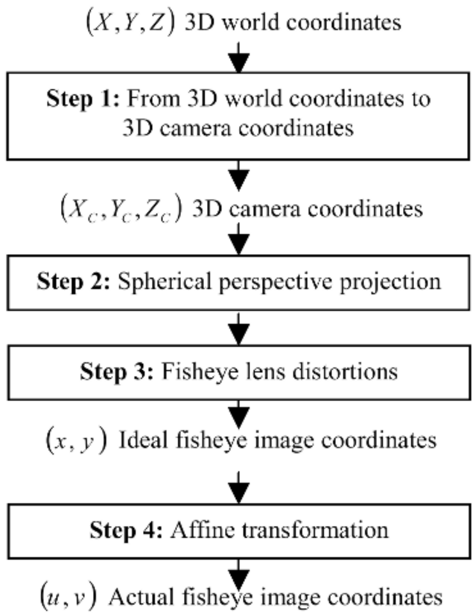

Fig. 2. Fisheye imaging model

$(X_C, Y_C, Z_C)^T$ are the coordinates in the camera coordinate system, the transformation between $\mathbf{P}_W$ and $\mathbf{P}_C$ is:

$$\mathbf{P}_C = \mathbf{R}\mathbf{P}_W + \mathbf{t}, \tag{1}$$

where the matrix **R** and vector **t** describe the orientation and position of the fisheye camera with respect to the world coordinate system. The parameters in **R** and **t** are called the extrinsic parameters.

Step 2: The space point is perspectively projected onto a unit sphere centered at the projection center. This procedure can be represented by a transformation from the 3D camera coordinates to the 2D spherical coordinates.

The unit sphere is called the viewing sphere. If **p** is the spherical projection of the space point, we have:

$$\mathbf{p} = \frac{\mathbf{P}_C}{\|\mathbf{P}_C\|} = (\sin \varPhi \cos \varTheta, \sin \varPhi \sin \varTheta, \cos \varPhi)^T, \tag{2}$$

where $\mathbf{p} = (\sin \varPhi \cos \varTheta, \sin \varPhi \sin \varTheta, \cos \varPhi)^T$ is the unit directional vector, and $(\varPhi, \varTheta)$ is the 2D spherical coordinates of the spherical point (see Fig. 3). Obviously, $(\varPhi, \varTheta)$ can be determined from **p**, and vice versa.

Step 3: The spherical projection point **p** is mapped to **m** on the image plane due to fisheye lens distortions, which can be represented as:

$$\mathbf{m} = D(\mathbf{p}), \tag{3}$$

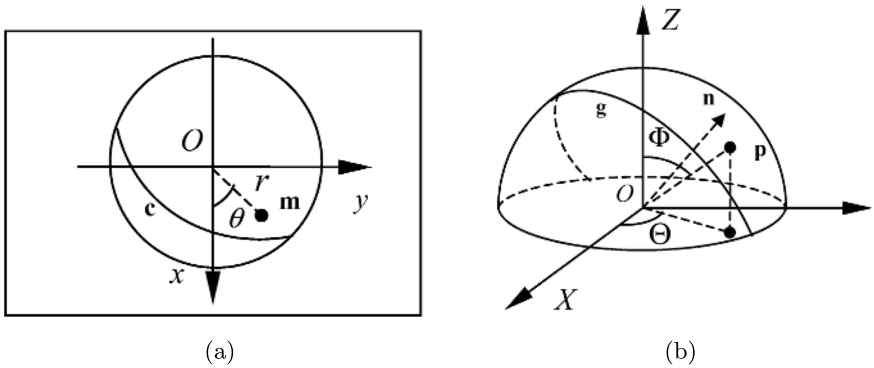

Fig. 3. (a) An ideal fisheye image. (b) The corresponding spherical perspective image. The spherical point **p** is mapped to **m** in the ideal fisheye image using the fisheye distortion model D. The great circle **g** which is the spherical projection of a straight line in space is mapped to a image curve **c** in the ideal fisheye image also using the fisheye distortion model D.

where $\mathbf{m} = (x, y)$, and D is the so-called fisheye distortion model. The image obtained here is called the ideal fisheye image. The parameters in D are called the distortion parameters. The fisheye distortion model will be discussed in details in the next section. Note that in Step 3, we obtain a planar image with the pixel coordinates, where the origin of the image coordinate system is located at the principal point, and the image coordinate system has equal scales in the directions of two coordinate axes.

Step 4: The image point **m** is transformed into $\mathbf{m}'$ using an affine transformation:

$$\mathbf{m}' = \mathbf{K}_A(\mathbf{m}), \tag{4}$$

where $\mathbf{m}' = (u, v)$. The image obtained here is called the actual fisheye image. The meaning of formula (4) is:

$$\tilde{\mathbf{m}}' = \mathbf{K}_A \tilde{\mathbf{m}}, \tag{5}$$

where $\tilde{\mathbf{m}} = (x, y, 1)^T$ and $\tilde{\mathbf{m}}' = (u, v, 1)^T$ are the homogeneous coordinates corresponding to **m** and $\mathbf{m}'$ respectively, and

$$\mathbf{K}_A = \begin{bmatrix} r & s & u_0 \\ 0 & 1 & v_0 \\ 0 & 0 & 1 \end{bmatrix}. \tag{6}$$

3 Fisheye Distortion Model

Fisheye distortion model D describes the mapping from a spherical perspective image to its corresponding ideal fisheye image (see Fig. 2 and Fig. 3). If **p** is the spherical perspective projection of a space point and (Φ, Θ) are the 2D spherical coordinates of $\mathbf{p}$, due to fisheye lens distortions, $\mathbf{p}$ is mapped to $\mathbf{m}$ in the ideal fisheye image. If (x, y) is the Cartesian coordinates and (r, θ) is the polar coordinates of where the origins of the two coordinate systems are both located at the principal point, the relation between (x, y) and (r, θ) is:

$$r = \sqrt{x^2 + y^2}, \tan\theta = \frac{y}{x}. \tag{7}$$

In our experiments, we use fifth degree polynomials to represent fisheye radial and tangential distortion models:

$$r = D_R(\Phi) = \sum_{i=1}^{5} d_i \Phi^i, \theta = D_T(\Theta) = \sum_{i=1}^{5} b_i \Theta^i, \tag{8}$$

where d_i are radial, and b_i are tangential distortion parameters. In fact, any other proper parametric distortion models for fisheye lenses can be employed, such as those proposed in [1, 3, 7, 8, 10, 11].

Since the FOV of fisheye lenses is known, we have:

$$\gamma = D_R(\frac{\alpha}{2}), \tag{9}$$

where γ is the radius of the ideal fisheye image, α is the fisheye lenses' FOV. After some manipulation, we have:

$$d_5 = \frac{32\gamma - 16\alpha d_1 - 8\alpha^2 d_2 - 4\alpha^3 d_3 - 2\alpha^4 d_4}{\alpha^5}. \tag{10}$$

So there are only four independent parameters for radial distortion. The longitude angle and the polar direction are both periodic. From $\Theta = 0$ and (8), we have $\theta = 0$. Therefore, if $\Theta = 2\pi$, then $\theta = 2\pi$. Thus we have:

$$b_5 = \frac{1 - b_1 - 2\pi b_2 - 4\pi^2 b_3 - 8\pi^3 b_4}{16\pi^4}. \tag{11}$$

So there are only four independent parameters for tangential distortion.

4 Fisheye Camera Calibration

From the discussions above, we know that there are totally 12 parameters for a fisheye lenses required to be calibrated: 4 affine transformation parameters, 4 radial and 4 tangential distortion parameters. These parameters are called the extended intrinsic parameters in this paper.

Given a fisheye image containing several image curves of space lines, we select a small set of points along these image curves. These sample points are mapped to spherical points on the viewing sphere using the concatenation of $\mathbf{K}_A^{-1}$ and D^{-1} , and the great circle fitting method is employed. The objective function is the sum of the squared distances of these spherical points from their corresponding best-fit great circles. In this section, we firstly introduce the algorithm for great circle fitting. Secondly, the objective function with the extended intrinsic parameters is constructed, and finally, how to find the initial values for these parameters is discussed.

4.1 Great Circle Fitting

A great circle is the intersection of a sphere and a plane passing through the spherical center. It can be determined by two parameters (α, β) which are the directional angles of the normal vector for the plane containing the great circle in the 3D Cartesian coordinate system whose origin is located at the spherical center (see Fig. 3b). For a spherical point $\mathbf{p}$ and a great circle $\mathbf{g} = (\alpha, \beta)$ where the unit normal vector for the plane containing the great circle is $\mathbf{n} = (\sin\alpha\cos\beta, \sin\alpha\sin\beta, \cos\alpha)^T$, the distance from $\mathbf{p}$ to the plane containing the great circle is $d = |\mathbf{p}^T\mathbf{n}|$. As noted in [6], the great circle fitting problem may be replaced by the problem of finding a plane so as to minimize the sum of squares of distances between the given points and the plane. Given N spherical points $\mathbf{p}_i$, the objective function is constructed as the sum of the squared distances of $\mathbf{p}_i$ from the plane containing the best-fit great circle:

$$F(\mathbf{n}) = \sum_{i=1}^{N} (\mathbf{p}_i^T\mathbf{n})^2, \tag{12}$$

where $\mathbf{n}$ is the normal vector for the plane. This can be converted into an eigenvalue problem. A vector equation is introduced as:

$$\mathbf{An} = 0, \tag{13}$$

where $\mathbf{A} = (\mathbf{p}_1, \mathbf{p}_2, \ldots, \mathbf{p}_N)^T$. The objective function becomes:

$$F(\mathbf{n}) = (\mathbf{An})^T\mathbf{An} = \mathbf{n}^T\mathbf{Bn}. \tag{14}$$

The solution for $\mathbf{n}$ is the eigenvector of $\mathbf{B}$ corresponding to the smallest eigenvalue. $\mathbf{g} = (\alpha, \beta)$ can be easily computed from the obtained $\mathbf{n}$.

4.2 Objective Function Formulation

We use L to represent the number of the sample image curves of space lines in the actual fisheye image, and use $N_j (j = 1, \ldots, L)$ to represent the number of the sample points on the j^{th} image curve. $\mathbf{m}'_{i,j} (j = 1, \ldots, L)$ represents the image coordinates of the sample point on the j^{th} image curve. The objective function can be constructed as:

$$\xi = \sum_{j=1}^{L} F(\mathbf{n}_j) = \sum_{j=1}^{L} \left[\sum_{i=1}^{N_j} (\mathbf{p}_{i,j}^T\mathbf{n}_j)^2 \right], \tag{15}$$

where $\mathbf{n}_j = (\sin\alpha_j\cos\beta_j, \sin\alpha_j\sin\beta_j, \cos\alpha_j)^T$ is the normal vector for the plane containing the best-fit great circle $\mathbf{g}_j = (\alpha_j, \beta_j)$, and

$$\mathbf{p}_{i,j} = D^{-1}(\mathbf{K}_A^{-1}(\mathbf{m}'_{i,j})), \tag{16}$$

where $\mathbf{p}_{i,j}$ represents the spherical point obtained from the sample image point $\mathbf{m}'_{i,j}$ after using the concatenation of $\mathbf{K}_A^{-1}$ and D^{-1} . The objective function ξ

describes the sum of the squared distances of $\mathbf{p}_{i,j}$ from its corresponding best-fit great circle $\mathbf{g}_j$. The Levenberg-Marquardt optimization technique is used to perform this minimization. The parameters for the great circles $\mathbf{g}_j = (\alpha_j, \beta_j)(j = 1, \ldots, L)$ are optimized together with the extended intrinsic parameters. As we know the initial values for the optimized parameters are required in the nonlinear minimization, therefore, the initial estimations of these parameters are discussed in the next section.

4.3 Initial Estimations

Affine Transformation Parameters. A significant characteristic of an actual fisheye image is that its boundary is usually an ellipse (see Fig. 1a). In fact, the bounding ellipse is the projection of the boundary between the optical components (glass lenses) and their metal supporting part. Light rays are occluded by the supporting part when the light rays are out of the fisheye camera FOV. The shape of the physical boundary is a circle. The optical axis of the fisheye camera is perpendicular to the plane containing the circle, and it also goes through the center of the circle. To identify the bounding ellipse of the fisheye image, we use a predefined threshold to find the boundary, and fit an ellipse to the resulting boundary. If the equation of the bounding ellipse is:

$$a'u^2 + 2b'uv + c'v^2 + 2d'u + 2e'v + f = 0, \tag{17}$$

we may obtain the initial values for affine transformation parameters as:

$$\begin{array}{cc} \overline{r} = \sqrt{-\frac{b'^2}{a'^2} + \frac{c'}{a'}} & \overline{s} = -\frac{b'}{a'} \\ \overline{u}_0 = \frac{b'e' - c'd'}{a'c' - b'^2} & \overline{v}_0 = \frac{b'd' - a'e'}{a'c' - b'^2} \end{array} . \tag{18}$$

Due to lack of space, the derivation is omitted here.

Distortion Correction Parameters. Since the equidistance model is a very good approximation to the real radial distortion of a fisheye camera [10], the initial values of the radial distortion correction parameters are set as: $\overline{c}_1 = \frac{\alpha}{2\gamma}$, and $\overline{c}_2 = \overline{c}_3 = \overline{c}_4 = 0.0$, where γ is the radius of the ideal fisheye image and α is the fisheye camera FOV. For the tangential distortion, the reasonable initial values are $\overline{a}_1 = 1.0, \overline{a}_2 = \overline{a}_3 = \overline{a}_4 = 0.0$ (i.e., $\Theta = \theta$).

Parameters of Best-Fit Great Circles. When the initial values for the extended intrinsic parameters have been obtained, we have:

$$\overline{\mathbf{p}}_{i,j} = \overline{D}^{-1}(\overline{\mathbf{K}}_A^{-1}(\mathbf{m}'_{i,j})), \tag{19}$$

where $\overline{\mathbf{K}}_A^{-1}$ and $\overline{D}^{-1}$ are $\mathbf{K}_A^{-1}$ and D^{-1} with the initial parameters respectively. $\overline{\mathbf{p}}_{i,j}$ represents the spherical point obtained from the sample image point $\mathbf{m}'_{i,j}$ after using the concatenation of $\overline{\mathbf{K}}_A^{-1}$ and $\overline{D}^{-1}$. From these spherical points $\overline{\mathbf{p}}_{i,j}$, the great circle fitting method described in Sect. 4.1 is used to fit great circles $\overline{\mathbf{g}}_j = (\alpha_j, \beta_j)(j = 1, \ldots, L)$ respectively. Therefore, the initial values for the parameters of the best-fit great circles are obtained.

5 Experiments

5.1 Simulations

We have performed a number of experiments with simulated data in order to assess the performances of our calibration algorithm. The extended intrinsic parameters $\{r, s, u_0, v_0, c_1, c_2, c_3, c_4, a_1, a_2, a_3, a_4\}$ for the simulated fisheye camera are generated randomly distributed within their corresponding valid ranges. The simulated fisheye lenses FOV is 180 degrees. The resolution of the image is 1024×1024. The generation procedure is constructed as follows: Firstly, the great circles are generated which representing the spherical projection of straight lines in space. Secondly, these great circles are transformed into image curves using D and $\mathbf{K}_A$. Thirdly, on each image curve about 50 points are chosen. Gaussian noise with zero-mean and σ standard deviation is added to these image points. The noise level σ is varied from 0.2 to 2.0 pixels. Finally, the ellipse boundary is also generated in the simulated fisheye image (see Fig. 4a).

In order to compare the recovered parameters with the ground truth, similar to [9], we use the reprojection error to evaluate the calibration accuracy:

$$\varepsilon_{rep} = \frac{1}{\sum_{j=1}^{L} N_j} \sum_{j=1}^{L} \left[\sum_{i=1}^{N_j} \|\mathbf{m}'_{i,j} - \mathbf{K}_A D(\widehat{D}^{-1} \widehat{\mathbf{K}}_A^{-1}(\mathbf{m}'_{i,j}))\| \right], \tag{20}$$

where $\mathbf{m}'_{i,j}$ are the coordinates of the sample points in the simulated fisheye image. $\mathbf{K}_A$ and D are with the ground truth. $\widehat{D}^{-1}$ and $\widehat{\mathbf{K}}_A^{-1}$ are with the recovered values. For each noise level, we perform 1000 independent trials, and the reprojection errors are computed over each run. The means and standard deviations of reprojection errors with respect to different noise levels are shown in Fig. 4b.

5.2 Real Images

The fisheye lenses used here is Nikon FC-E8 with FOV 183 degrees, mounted on a Nikon COOLPIX 990 digital camera. A fisheye image taken with this fisheye

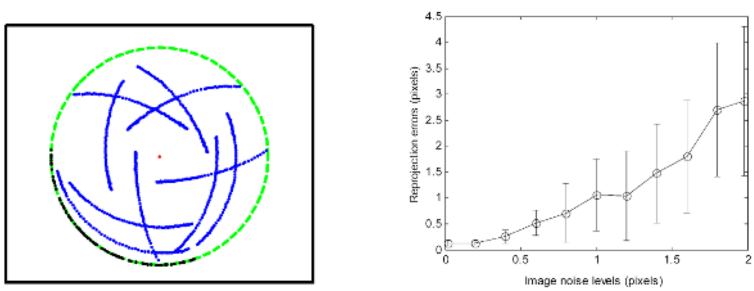

(a) (b)

Fig. 4. Simulation results for fisheye calibration. (a) A simulated fisheye image containing image curves of straight lines in space. (b) The means and the standard deviations of the reprojection errors with respect to different noise levels.

Table 1. The mean and maximum of the reprojection errors for the three planar homographies. The errors shown here are divided by the side length of a square grid.

	Mean error	Max. error
$\{\mathbf{x} \leftrightarrow \mathbf{q}_1\}$	76.44%	246.92%
$\{\mathbf{x} \leftrightarrow \mathbf{q}_2\}$	13.21%	40.96%
$\{\mathbf{x} \leftrightarrow \mathbf{q}_3\}$	1.64%	3.08%

camera for calibration is shown in Fig. 1a. The resolution of the fisheye image is 2048×1536. From this fisheye image, about 10 image curves of the straight lines in space and total about 500 sample points are chosen. The extended intrinsic parameters of the fisheye camera are recovered using our calibration method. Then, we apply these recovered parameters to undistort the fisheye image, and the spherical perspective image is obtained as shown in Fig. 1b.

Here, we use planar homography constraint to evaluate calibration accuracy. We select some fisheye images of grid points on a ceiling in Fig. 1a. There are totally three sets of point pairs for evaluating the homography constraint: $\{\mathbf{x} \leftrightarrow \mathbf{q}_1\}$, $\{\mathbf{x} \leftrightarrow \mathbf{q}_2\}$ and $\{\mathbf{x} \leftrightarrow \mathbf{q}_3\}$, where $\mathbf{q}_1$ represents the 2D homogeneous coordinates of the fisheye image point, $\mathbf{q}_2$ represents the unit directional vector of the spherical point obtained using the distortion correction procedure with the initial values of the extended intrinsic parameters, and $\mathbf{q}_3$ similar to $\mathbf{q}_2$ but with the recovered values. The reprojection error to evaluate homography constraint is:

$$\varepsilon_i = \|\mathbf{x} - \mathbf{H}_i^{-1}\mathbf{q}_i\|, i = 1, 2, 3, \tag{21}$$

where $\mathbf{H}_i (i = 1, 2, 3)$ is the obtained planar homography. The mean and maximum of the reprojection errors are shown in Table 1. From Table 1, we can see that the improvement of the planar homography constraint is very significant due to the fisheye lenses distortion correction.

6 Conclusions

In this paper, we propose a novel calibration method for fisheye lenses using the images of space lines. The SLSPPC is employed for calibrating fisheye lenses with FOV around 180 degrees, whereas the existing methods based on SLPPPC cannot be used in this case. The extended intrinsic parameters of fisheye cameras can be calibrated without needing to seek the extrinsic parameters. Thus, the number of parameters to be calibrated is drastically reduced, making the calibration procedure simple and practical. Our method can use any other suitable parametric distortion models for fisheye lenses though we only use the polynomial models here.

Acknowledgements

This work was supported in part by the NSFC Grant (No. 60333010), and NKBRPC (No. 2004CB318000).

References

1. A. Basu and S. Licardie: Alternative models for fish-eye lenses, Pattern Recognition Letters, 16(4), 1995, pp. 433-441
2. D.C. Brown: Close range camera calibration. Photogrammetric Engineering, 37(8): pp.855-866, 1971
3. D.C. Brown: Decentering distortion of lenses. Photogrammetric Engineering,32(3), 1966, pp. 444-462
4. F. Devernay, O. Faugeras: Straight Lines Have to Be Straight: Automatic Calibration and Removal of Distortion from Scenes of Structured Environments, Machine Vision and Applications, 2001, vol.1, pp.14-24
5. S. B. Kang: Radial distortion snakes, IAPR Workshop on MVA, 2000, pp. 603-606
6. C. F. Marcus: A note on fitting great circles by least squares, Communications of the ACM, 4(11), 1961
7. B. Micusik and T. Pajdla: Estimation of Omnidirectional Camera Model from Epipolar Geometry, CVPR, 2003
8. S. Shah, J. K. Aggarwal: Intrinsic Parameter Calibration Procedure for a (High Distortion) Fish-Eye Lens Camera with Distortion Model and Accuracy Estimation. Pattern Recognition, 1996, vol.29, no.11, pp.1775-1788
9. R. Swaminathan, S.K. Nayar: Non-Metric Calibration of Wide-Angle Lenses and Polycameras. PAMI, 2000, pp. 1172-1178
10. Y. Xiong, K. Turkowski: Creating Image-Based VR Using a Self-Calibrating Fisheye Lens. Proceedings of CVPR, 1997, pp. 237-243
11. X. Ying, Z. Hu: Can We Consider Central Catadioptric Cameras and Fisheye Cameras within a Unified Imaging Model. Proceedings of ECCV, 2004(1), pp. 442-455